PHYSICAL REVIEW C **75**, 041301(R) (2007)

High-spin lifetime measurements in the $N = Z$ nucleus ^{72}Kr

C. Andreoiu,[1,2] C. E. Svensson,[1] A. V. Afanasjev,[3] R. A. E. Austin,[4,*] M. P. Carpenter,[5] D. Dashdorj,[6] P. Finlay,[1] S. J. Freeman,[5] P. E. Garrett,[1] J. Greene,[5] G. F. Grinyer,[1] A. Görgen,[7] B. Hyland,[1] D. Jenkins,[8] F. Johnston-Theasby,[8] P. Joshi,[8] A. O. Machiavelli,[9] F. Moore,[5] G. Mukherjee,[5] A. A. Phillips,[1] W. Reviol,[10] D. G. Sarantites,[10] M. A. Schumaker,[1] D. Seweryniak,[5] M. B. Smith,[11] J. J. Valiente-Dobón,[1,†] and R. Wadsworth[8]

[1]*Department of Physics, University of Guelph, Guelph, Ontario, Canada N1G 2W1*

[2]*Oliver Lodge Laboratory, University of Liverpool, Liverpool L69 3BX, United Kingdom*

[3]*Department of Physics and Astronomy, Mississippi State University, Starkville, Mississippi 39762, USA*

[4]*McMaster University, Hamilton, Ontario, Canada L8S 4K1*

[5]*Physics Division, Argonne National Laboratory, Argonne, Illinois 60436, USA*

[6]*North Carolina State University, Raleigh, Norht Carolina 27695, USA*

[7]*CEA Saclay, Daphnia/SphN, F-91191 Gif-sur-Yvette Cedex, France*

[8]*Department of Physics, University of York, Heslington, York YO10 5DD, United Kingdom*

[9]*Lawrence Berkeley National Laboratory, Berkeley, California 94720, USA*

[10]*Department of Chemistry, Washington University, St. Louis, Missouri 63130, USA*

[11]*TRIUMF, 4004 Wesbrook Mall, Vancouver, British Columbia, Canada V6T 2A3*

(Received 23 November 2005; revised manuscript received 20 December 2006; published 11 April 2007; corrected 19 April 2007)

High-spin states in the $N = Z$ nucleus ^{72}Kr have been populated in the ^{40}Ca(^{40}Ca, 2α)^{72}Kr fusion-evaporation reaction at a beam energy of 165 MeV using the Gammasphere array for γ-ray detection coupled to the Microball array for charged particle detection. The previously observed bands in ^{72}Kr were extended to an excitation energy of $\sim$24 MeV and angular momentum of $30\hbar$. Using the Doppler shift attenuation method the lifetimes of high-spin states were measured for the first time. Excellent agreement between the results of calculations within the isovector mean field theory and experiment is observed both for rotational and deformation properties. No enhancement of quadrupole deformation expected in the presence of isoscalar $t = 0$ *np* pairing is observed. Current data do not show any evidence for the existence of the isoscalar *np* pairing.

DOI: 10.1103/PhysRevC.75.041301 PACS number(s): 23.20.Lv, 27.50.+e, 21.10.Re, 21.60.Ev

Nuclei with an equal number of protons and neutrons ($N = Z$) are of particular interest regarding *np* correlations, that are expected to be significant in these nuclei due to the large spacial overlap of proton- and neutron-wave functions. These correlations can have either an isoscalar or an isovector character, and in principle might form a static pair condensate in either channel. Experimental evidence from pair-transfer reactions [1], binding energy systematics [2,3] and symmetry properties of rotational excitations [4] establish an isovector ($t = 1$) pair field in $N \approx Z$ nuclei with a magnitude consistent with that expected from the systematics of $t = 1$ *nn* and *pp* pair gaps throughout the chart of the nuclides. Isospin symmetry requires that the strength of the $t = 1$ *np* pairing is equal to the strength of the *nn* and *pp* pairing [5]. The situation concerning the role of $t = 0$ *np* pairing in $N = Z$ nuclei is less clear. The ground-state binding energy systematics leave little room for a collective $t = 0$ pair gap [3]; a result understood in terms of the disruptive influence of the spin-orbit splitting on $t = 0$ *np* pairing [6,7], and consistent with the analysis [8] of pairing vibrations around ^{56}Ni which indicates that the effective $t = 0$ pairing strength represents only a small fraction ($\sim$0.2) of the critical value required for condensate formation.

Considering the complicated nature of the problem, the search for signals of isoscalar $t = 0$ *np*-pairing via other physical observables is of paramount importance. For some period of time, it was thought that the rotational properties such as moments of inertia and band crossing frequencies can provide sufficient evidence for the existence of $t = 0$ *np*-pair condensate (see review of the situation in Ref. [9]). However, systematic analysis of these properties in the $N \approx Z$ nuclei of the $A = 58$–80 mass region showed that they are well understood in the framework of isovector mean field theory [5], which assumes that isoscalar *np* pairing is absent, provided that the shape changes and the effects associated with band termination are taken into account [9]. It turns out that little attention has been paid to the deformation properties of rotational structures and their relation to the existence of the isoscalar *np*-pairing. In particular, the prediction of Ref. [10] that $t = 0$ *np*-pairing enhances the quadrupole deformation has not been tested. In order to test if this prediction is valid or not, it is necessary (i) to compare theoretical and experimental results for transition quadrupole moments both for the $N = Z$ nucleus and the nucleus which is not expected to be affected by the $t = 0$ *np*-pairing, (ii) to see if the calculations are able to reproduce the impact of single particles on deformation properties in the $N = Z$ system. ^{72}Kr is very good choice for such a study since (i) transition quadrupole moments were measured (and compared with calculations) in three bands of ^{74}Kr and (ii) that several bands are available in this nucleus.

*Present address: Saint Mary's University, Halifax, Nova Scotia B3H 3C3, Canada.

†Present address: INFN, Laboratori Nazionali di Legnaro, I-35020, Legnaro, Italy.

The experiment, performed at Argonne National Laboratory, employed the ^{40}Ca(^{40}Ca,2α)^{72}Kr fusion-evaporation reaction at a beam energy of 165 MeV. The 0.350 mg/cm^2 thin isotopically enriched ^{40}Ca target was placed between two 150 μg/cm^2 thin layers of Au to prevent oxidation. The experimental setup consisted of the Gammasphere array [11], at the time comprised off 99 Compton-suppressed HPGe detectors in combination with the 95-element CsI(Tl) Microball detector [12]. The event trigger required the detection of at least four Compton suppressed γ rays. To provide γ-ray multiplicity and sum-energy measurements [13], and additional selectivity by total energy conservation requirements [14] the Hevimet collimators were removed from the Gammasphere detectors. Based on the charged-particle energies and directions detected in Microball, the momenta of the recoiling residual nuclei were determined for each event, allowing for a more accurate Doppler-shift correction of the γ-ray energies, leading to a significantly improved energy resolution. The events were sorted off-line into various E_γ projections, E_γ-E_γ matrices, and E_γ-E_γ-E_γ cubes by selecting events in which 2α particles corresponding to ^{72}Kr were detected in Microball. The events belonging to the 2α1p channel populating ^{71}Br were carefully suppressed from this data set by the total energy conservation requirements.

The main focus of this work was determining the lifetimes of high-spin states using the centroid-shift Doppler shift attenuation method [15]. The states at the top of the rotational bands have lifetimes of the order of tens of femtoseconds, thus they decay while the recoils are slowing down in the thin ^{40}Ca target. A Doppler correction was applied to the events with a recoil velocity β_0 corresponding to the velocity of the ^{72}Kr recoil at the time of formation as deduced on an event-by-event basis from the measured evaporated charged particles. As a result, the peaks are slightly shifted in the γ-ray spectra of the Germanium detectors at forward and backward angles. From the shift measurement the mean velocity, β_t, at the time when the transition was emitted was obtained. The fractional Doppler shift defined as $F(\tau) = \beta_t/\beta_0$ for each transition was experimentally obtained and plotted as a function of angular momentum. These $F(\tau)$ values were fit to extract the best transitional quadrupole moment Q_t for each band. The code used to determine the Q_t's takes into account the initial momenta of the ^{72}Kr recoil and a velocity history of the ^{72}Kr recoils including their directions in time steps of 0.05 fs. The beam and recoil stopping power in the target were simulated using the SRIM-2003 code [16]. The boost given to the recoil by the 2α particle evaporation were accounted for in the off-line analysis. Additional experimental details can be found in Refs. [17,18].

Previously high-spin states in ^{72}Kr were known up to an angular momentum of 28$\hbar$ [19]. Figure 1 shows the level scheme of ^{72}Kr obtained from the present experiment. The level scheme was extended up to an excitation energy of ~24 MeV and an angular momentum of 30$\hbar$.

Previous to this study no lifetimes of high-spin states were measured. The value of a transition quadrupole moment of 1.15(15) eb given in Ref. [19] for band 4 at spin 22$\hbar$ is only an estimate. The experimental $F(\tau)$ values of band 2 and 4 and the side band, as a function of angular momentum are

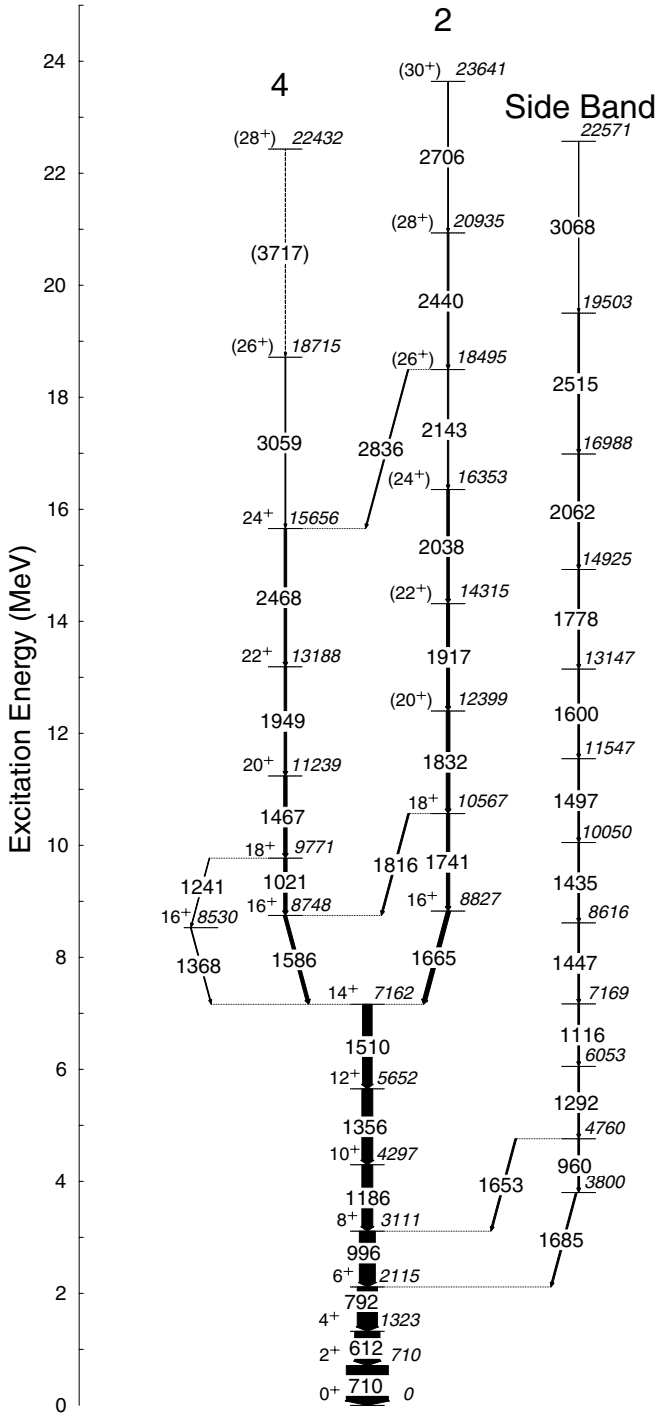

FIG. 1. Proposed high-spin level scheme of ^{72}Kr from the present experiment. Energy labels are in keV. The widths of the arrows are proportional to the relative intensities of the γ rays. Tentative transitions are dashed.

shown in Fig. 2. In order to extract a quadrupole moment from these measurements, the decay of the band was modeled assuming a constant in-band Q_t and the feeding of the band and the slowing down of the recoils in the target were treated as in Ref. [20]. The best fit to the data is obtained with $Q_t = 2.76(^{28}_{22})\,e$b for band 2, $Q_t = 2.00(^{36}_{28})\,e$b for band 4,

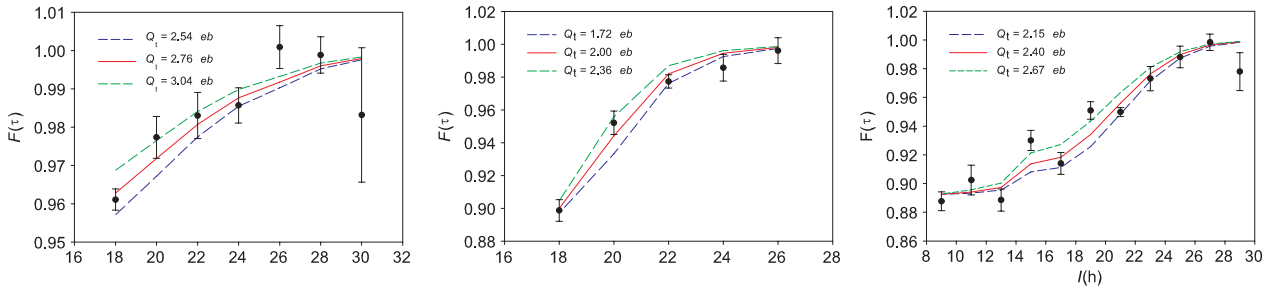

FIG. 2. (Color online) Experimental $F(\tau)$ values (symbols) and transition quadrupole moments Q_t (lines), for band 2, 4, and side band as a function of angular momentum are shown in the right panel, middle panel, and lower panel, respectively. The solid curves represent the best least-square fits to the data points and correspond to an average quadrupole moment of 2.76 eb for band 4, 2.00 eb for band 2, and 2.40 eb for the side band, respectively. The dashed lines mark the quadrupole moments for which $\chi^2_{\rm red} = \chi^2_{\rm red,min} + 1$.

and $Q_t = 2.40(^{26}_{23})e$b for the side band. In the right panel of Fig. 2 the discontinuity in the fit curve for the side band at the 8616 keV level results from the combination of the fact that the 1447 keV transition is actually higher energy than the 1435 keV transition, which makes it faster for the same quadrupole moment, and there is also some significant side feeding into the 8616 keV level. Also the apparent "staggering" of the data points is just statistical fluctuations. The uncertainties in the quadrupole moments do not include the systematic uncertainties due to the stopping power, which are typically 10%. It is clear from the results that band 2 has a higher Q_t than band 4. With the current experimental uncertainties on the $F(\tau)$ measurements, investigations with variable Q_t's do not provide a significantly better description of the bands.

Isovector mean field theory [5] assumes that there is no isoscalar *np* pairing, but takes into account isovector *np* pairing and isospin symmetry conservation. An advantage of this approach is the fact that standard mean field models with only $t = 1$ like-particle pairing (or even without it at high spin) can be employed. Thus, theoretical calculations for ^{72}Kr have been performed with cranked Nilsson Strutinsky (CNS) [21], the cranked relativistic mean field (CRMF) [22], and the cranked relativistic Hartree-Bogoliubov (CRHB) [23] approaches. Some of these results were previously reported in Ref. [9]. Pair correlations are neglected in the CNS and CRMF calculations, so these calculations can be compared with experiment only at spin above $\sim 15\hbar$, where pairing is expected to be negligible. The standard set of Nilsson parameters [24] is used in the CNS calculations. The NL3 parametrization of the relativistic mean-field Lagrangian [25] is employed in CRMF and CRHB calculations. The D1S Gogny force [26] is used in the pairing channel of the CRHB theory [23]. In addition, approximate particle number projection is performed by means of the Lipkin-Nogami (LN) method in the CRHB framework. In the calculations without pairing, the bands are labeled by the number of $g_{9/2}$ protons and neutrons, as $[p, n]$.

Figure 3 shows the experimental excitation energies minus a rigid rotor reference versus angular momentum for bands 2 and 4 and the corresponding theoretical configurations. In Ref. [9] band 4 was assigned to the [2,2] configuration (i.e., the double S-band).

The CNS and CRMF calculations indicate the presence of two closely lying [3,3] configurations (Fig. 3), which are the candidates for the band 2. The configurations [3,3]a and [3,3]b are obtained from the [2,2] configuration by exciting a proton and a neutron from the $3_3(\alpha = -1/2)$ and $3_3(\alpha = +1/2)$ orbitals into second $g_{9/2}(\alpha = +1/2)$ orbital, respectively. The details of the interpretation of band 2 are, however, somewhat model dependent reflecting the fact that the description of the energies of the single-particle states is not optimal. The CNS calculations with the Nilsson parameters from Ref. [27] ('A80' parameters) and the CRMF calculations are similar and they suggest that the band 2 may be the envelope of the [3,3]a and [3,3]b configurations (see top panel in Fig. 3), whereas the CNS calculations with the standard Nilsson parameters suggests the [3,3]a configuration. In the former case the irregularities

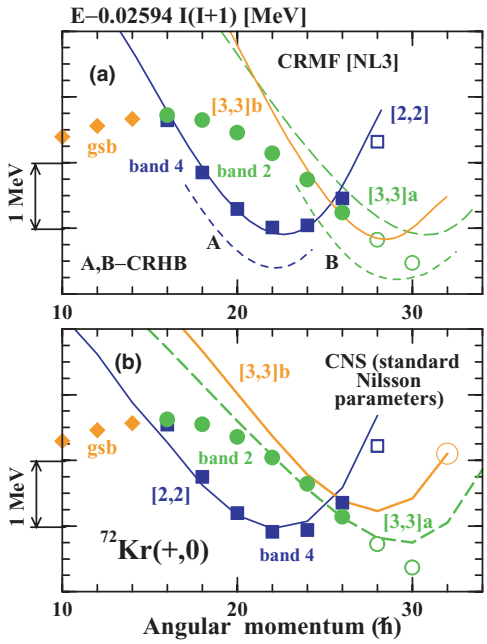

FIG. 3. (Color online) Excitation energies of the experimental bands 2 and 4 and theoretical configurations calculated in (a) the CRMF, CRHB, and (b) CNS approaches relative to a rigid rotor reference $E_{\rm RLD} = E - 0.02594I(I + 1)$. Experimental data are shown by symbols, while lines are used for theoretical results. The ground state band is indicated as 'g.s.b.'. Open symbols are used for the states observed for the first time in the present manuscript.

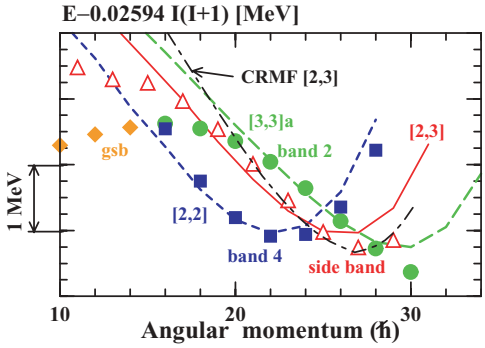

FIG. 4. (Color online) Excitation energies relative to a rigid rotor reference $E_{\mathrm{RLD}} = E - 0.02594I(I+1)$. Experimental bands 2, 4, and side band and the results of the CNS calculations (with the standard parameters for the Nilsson potential) for their theoretical counterparts are shown. In addition, the CRMF [2,3] configuration is shown by dash-dotted line.

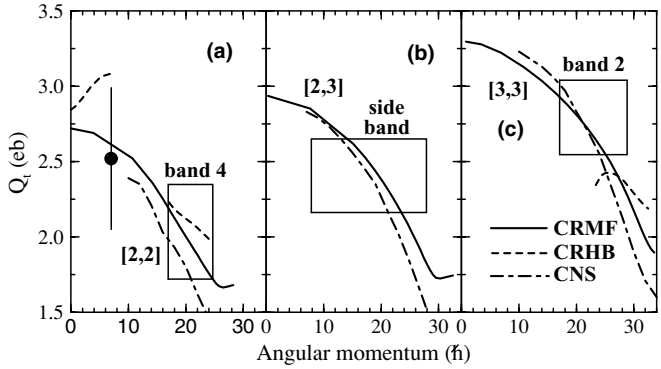

FIG. 5. Transition quadrupole moments as a function of angular momentum for (a) band 4, (b) side band, and (c) band 2. The data point at $I = 8\hbar$ is from Ref. [30], while boxes represent the measured transition quadrupole moments and their uncertainties within the measured spin range from the present work. The results of the calculations are shown by the lines.

seen in $J^{(2)}$ of the band 2 at $\omega \geqslant 0.8$ MeV (see Fig. 2 in Ref. [28]) may be explained as due to the crossing of the [3,3]a and [3,3]b configurations. However, a number of factors favors the assignment of the [3,3]a configuration to the band 2. An analysis of the relative energies of experimental bands in ^{73,74}Kr and ^{70}Br shows that they are better described in the CNS calculations with the standard set of the Nilsson parameters as compared with the ones employing 'A80' parameters. The experimental $E - E_{\mathrm{RLD}}$ plot at spin larger than $20\hbar$ is better described by the [3,3]a configuration (see Fig. 3). Figure 4 shows the experimental excitation energies minus a rigid rotor reference versus angular momentum of the band 4, side band and band 2, and the results of the CNS calculations with the standard Nilsson parameters for their theoretical counterparts, and with the CRMF [2,3] configuration. The transition quadrupole moment Q_t of the configuration [3,3]b is smaller than the one of the [3,3]a configuration by 0.5–0.75 eb in the spin range of interest (see Fig. 11 in Ref. [9]). While the [3,3]a configuration reproduces the observed values of Q_t of band 2 reasonably well (Fig. 5), the same will not be possible if the configuration [3,3]b is assigned to band 2.

The CRHB calculations were performed for the configurations A and B which are the paired analogs of unpaired [2,2] and [3,3]a configurations (Fig. 3). Their energies are lower than those of their unpaired analogs by approximately 0.7 MeV. The pairing correlations in these configurations are small. As a consequence of weak pairing correlations, the results of the CRHB calculations are very close to the ones of CRMF for the physical observables of interest such as $(E - E_{\mathrm{RLD}})$ plots (Fig. 3) (and, as a result, kinematic and dynamic moments of inertia), and transition quadrupole moments (Fig. 5). Side band is linked to the ground state band by the 1685 and 1653 keV transitions of unknown multipolarity. If one assumes $E2$ multipolarity for these transitions, then this band would have parity $\pi = +$ and signature $r = 0$. With this assignment, all observed high-spin bands would have the same parity-signature contrary to theoretical results obtained in the CNS and CRMF calculations which suggest the presence of near-yrast rotational sequences of negative parity (see Fig. 4). Thus, $E1$ multipolarity is more likely choice for the multipolarities of these transitions. With this assignment, side band has negative parity and extends from spin 7^- up to spin 29^- and is well described by the [2,3] configuration in the CNS and CRMF calculations at spin $I \geqslant 17\hbar$ (Fig. 4). The relative energies of the band 4, side band and band 2 are well described in the CNS calculations with the standard Nilsson parameters by the [2,2], [2,3] and [3,3] configurations (see Fig. 4).

Figure 5 compares measured transition quadrupole moments of observed bands with the ones of assigned configurations. Starting from the [2,2] configuration (band 4), subsequent additions of $g_{9/2}$ particle(s) increase the transition quadrupole moment. This trend is seen both in calculations and experiment. In addition, absolute values of Q_t are well described in the calculations. Experimental data on transition quadrupole moments are also available for ^{74}Kr [29]. These data (both absolute values and relative changes in Q_t) agree rather well with the results of the CNS, CRMF, and CRHB calculations (see Refs. [9,29] for details). Comparing the experimental Q_t values in ^{72,74}Kr nuclei between each other and with the results of theoretical calculations, one can conclude that *no enhancement of quadrupole deformation in the $N = Z$ nuclei (which is expected in the presence of $t = 0$ np-pairing* [10]*) is required in order to reproduce experiment within the framework of isovector mean field theory.* The data on transition quadrupole moments are also available in superdeformed rotational bands in $N = Z + 1$ ^{59}Cu [31] and $N = Z$ ^{60}Zn [32] nuclei. Being less extensive as compared with ^{72,74}Kr data, it also supports this conclusion since it is well reproduced by the same theoretical tools [31,33].

An experiment to populate high-spin states in the $N = Z$ nucleus ^{72}Kr was performed with Gammasphere and Microball. The level scheme was extended up to an excitation energy of ~24 MeV and an angular momentum of $30\hbar$. The lifetimes of high-spin states were measured for the first time using the DSAM method and transitional quadrupole moments for each band were determined. The experiment is in good agreement with theoretical calculations within the framework

of isovector mean field theory. Thus, no clear signal of $t = 0$ *np* pairing can be found.

The authors thank I. Ragnarsson for useful discussions. This research was partially supported by the National Science and Engineering Research Council of Canada, the U.K. Engineering and Physical Sciences Research Council, and the U.S. Department of Energy under Contract Nos. DE-AC03-76SF00098, DE-FG02-88ER-40406, DE-FG03-03NA0076, DE-FG02-07ER41459, and DE-AC02-06CH11357. C. A. acknowledges the support offered by the Swedish Foundation for Higher Education and Research and the Swedish Research Council.

[1] D. R. Bes, R. A. Broglia, O. Hansen, and O. Nathan, Phys. Rep. **34**, 1 (1977).
[2] P. Vogel, Nucl. Phys. **A662**, 148 (2000).
[3] A. O. Macchiavelli *et al*., Phys. Rev. C **61**, 041303(R) (2000).
[4] C. D. O'Leary *et al*., Phys. Rev. C **67**, 021301(R) (2003).
[5] S. G. Frauendorf and J. A. Sheikh, Nucl. Phys. **A645**, 509 (1999).
[6] A. Poves and G. Martinez-Pinedo, Phys. Lett. **B430**, 203 (1998).
[7] O. Juillet and S. Josse, Eur. Phys. J. A **8**, 291 (2000).
[8] A. O. Macchiavelli *et al*., Phys. Lett. **B480**, 1 (2000).
[9] A. V. Afanasjev and S. Frauendorf, Phys. Rev. C **71**, 064318 (2005).
[10] J. Terasaki, R. Wyss, and P.-H. Heenen, Phys. Lett. **B437**, 1 (1998).
[11] I.-Y. Lee, Nucl. Phys. **A520**, 641c (1990).
[12] D. G. Sarantites *et al*., Nucl. Instrum. Methods Phys. Res. A **381**, 418 (1996).
[13] M. Devlin, L. G. Sobotka, D. G. Sarantites, and D. R. LaFosse, Nucl. Instrum. Methods Phys. Res. A **383**, 506 (1996).
[14] C. E. Svensson *et al*., Nucl. Instrum. Methods Phys. Res. A **396**, 228 (1997).
[15] B. Cederwall *et al*., Nucl. Instrum. Methods Phys. Res. A **354**, 591 (1995).
[16] J. F. Ziegler, http://www.srim.org
[17] J. J. Valiente-Dobón *et al*., Phys. Rev. C **71**, 034311 (2005).
[18] C. Andreoiu *et al*., Phys. Scr. T **125**, 127 (2006).
[19] S. M. Fischer, C. J. Lister, and D. P. Balamuth, Phys. Rev. C **67**, 064318 (2003).
[20] C. E. Svensson *et al*., Phys. Rev. Lett. **79**, 1233 (1997).
[21] A. V. Afanasjev, D. B. Fossan, G. J. Lane, and I. Ragnarsson, Phys. Rep. **322**, 1 (1999).
[22] A. V. Afanasjev, J. König, and P. Ring, Nucl. Phys. **A608**, 107 (1996).
[23] A. V. Afanasjev, P. Ring, and J. König, Nucl. Phys. **A676**, 196 (2000).
[24] T. Bengtsson and I. Ragnarsson, Nucl. Phys. **A436**, 14 (1985).
[25] G. A. Lalazissis, J. König, and P. Ring, Phys. Rev. C **55**, 540 (1997).
[26] J. F. Berger, M. Girod, and D. Gogny, Comput. Phys. Commun. **63**, 365 (1991).
[27] D. Galeriu, D. Bucurescu, and M. Ivaşcu, J. Phys. G **12**, 329 (1986).
[28] S. M. Fischer *et al*., Phys. Rev. Lett. **87**, 132501 (2001).
[29] J. J. Valiente-Dobón *et al*., Phys. Rev. Lett. **95**, 232501 (2005).
[30] G. de Angelis *et al*., Phys. Lett. **B415**, 217 (1997).
[31] C. Andreoiu *et al*., Phys. Rev. C **62**, 051301(R) (2000).
[32] C. E. Svensson *et al*., Phys. Rev. Lett. **82**, 3400 (1999).
[33] A. V. Afanasjev, I. Ragnarsson, and P. Ring, Phys. Rev. C **59**, 3166 (1999).